Title

Kinetic Pathways Templated by Low-Temperature Intermediates during Solid-State Synthesis of Layered Oxides

Journal

Chemistry of Materials, 32(23)

ISSN

0897-4756

Authors

Bai, J
Sun, W
Zhao, J
et al.

Publication Date

2020-12-08

DOI

10.1021/acs.chemmater.0c02568

Peer reviewed

CHEMISTRY OF MATERIALS

pubs.acs.org/cm Article

Kinetic Pathways Templated by Low-Temperature Intermediates during Solid-State Synthesis of Layered Oxides

Jianming Bai, Wenhao Sun, Jianqing Zhao, Dawei Wang, Penghao Xiao, Jun Young Peter Ko, Ashfia Huq, Gerbrand Ceder,* and Feng Wang*

Cite This: *Chem. Mater.* 2020, 32, 9906–9913 Read Online

ACCESS | Metrics & More | Article Recommendations | Supporting Information

ABSTRACT: Layered oxides have been the dominant cathodes in lithium-ion batteries, and among them, high-nickel (Ni) systems are attractive because of their high capacity. For practical use, synthetic control of stoichiometry and structural ordering is crucial but has been nontrivial due to the complexity inherent to synthesis reactions, which often proceed *via* nonequilibrium pathways. We report here a combined *in situ* synchrotron X-ray diffraction and *ab initio* study of solid-state synthesis of layered oxides starting from acetate precursors for $LiCoO_2$ and $LiNiO_2$ and their solid solution $LiNi_{0.8}Co_{0.2}O_2$. While all three systems ultimately evolve into the same thermodynamically stable layered phase ($R\bar{3}m$), each chemistry involves distinct metastable intermediates. We explain the phase progressions using a structural template model, demonstrating that during the synthesis of $LiCoO_2$, the formed metastable spinel polymorph ($Li_2Co_2O_4$; $Fd\bar{3}m$) is a kinetically facile lithiation product of spinel Co_3O_4—the low-temperature (LT) intermediate from the decomposed Co-acetate. Similarly, in the Ni-based systems, the acetate decomposition products, rocksalts (Ni,Co)O, topotactically template the kinetic pathways of forming disordered rocksalts ($Li_x(Ni,Co)_{2-x}O_2$; $Fm\bar{3}m$), consequently leading to off-stoichiometric $Li_x(Ni,Co)O_2$ with undesired high Li/Ni mixing. These findings highlight new opportunities for engineering precursors to form LT intermediates that template the synthesis of target phases and structural properties.

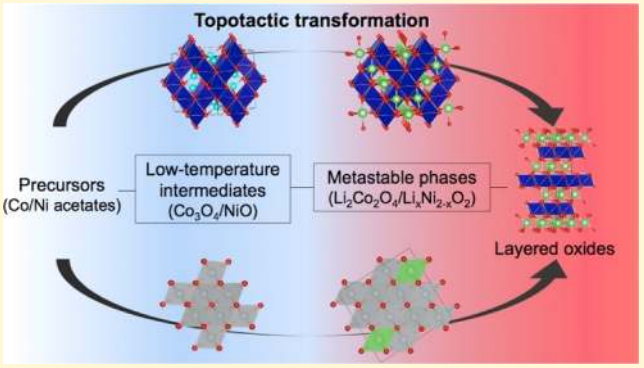

1. INTRODUCTION

Transition-metal layered oxides with a hexagonal structure (space group $R\bar{3}m$) have been the dominant cathodes for lithium-ion batteries (LIBs) over the past three decades.[1,2] Such layered oxides are typified by $LiCoO_2$ (LCO) and $LiNiO_2$ (LNO) as well as their solid-solutions with other metal species including Mn and Al.[3,4] In particular, high-Ni compositions such as $LiNi_xM_{1-x}O_2$ (M = Co, Mn, $x > 0.7$) exhibit high energy density and have emerged as the most promising cathodes for LIBs.[5] However, the electrode performance of these layered oxides is often compromised by poor stoichiometry control and interlayer Li/metal mixing during the solid-state synthesis of these materials.[6] Understanding the thermodynamics and kinetics of phase evolution during synthesis is crucial toward optimizing the performance of these important cathode materials.

For LCO, LNO, and $LiNi_{1-x}M_xO_2$, the layered $R\bar{3}m$ phase is the thermodynamically stable polymorph.[7] However, nonequilibrium structural intermediates are often observed during the solid-state synthesis of these compounds. For example, synthesis of LCO at low temperatures (LTs) often results in the formation of a spinel-type $Li_2Co_2O_4$ polymorph with $Fd\bar{3}m$ symmetry, which offers less capacity compared to the layered phase.[8−10] Because this spinel $Li_2Co_2O_4$ phase is observed to form predominantly at LTs, it is usually referred to as LT-LCO.[11]

However, first-principles investigations of LCO phase stability show that the spinel LT-LCO is actually metastable with respect to the layered phase at all temperatures,[12,13] prompting questions about the mechanistic origin of its formation. In LNO and $LiNi_{1-x}M_xO_2$, a metastable disordered layered compound with Li/Ni mixing can arise.[14] This cation disordering is considered a crucial issue, leading to low capacity and poor cycling stability in Ni-based cathodes.[15,16] The disordering may have been introduced upon formation of the layered phase,[17] therefore making the synthesis of structurally ordered layered oxides difficult, especially when multiple transition metals are involved.[18] Additional challenge comes from the fact that transition-metal ordering is highly

Received: June 19, 2020
Revised: September 15, 2020
Published: September 17, 2020

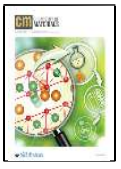

https://dx.doi.org/10.1021/acs.chemmater.0c02568
Chem. Mater. 2020, 32, 9906−9913

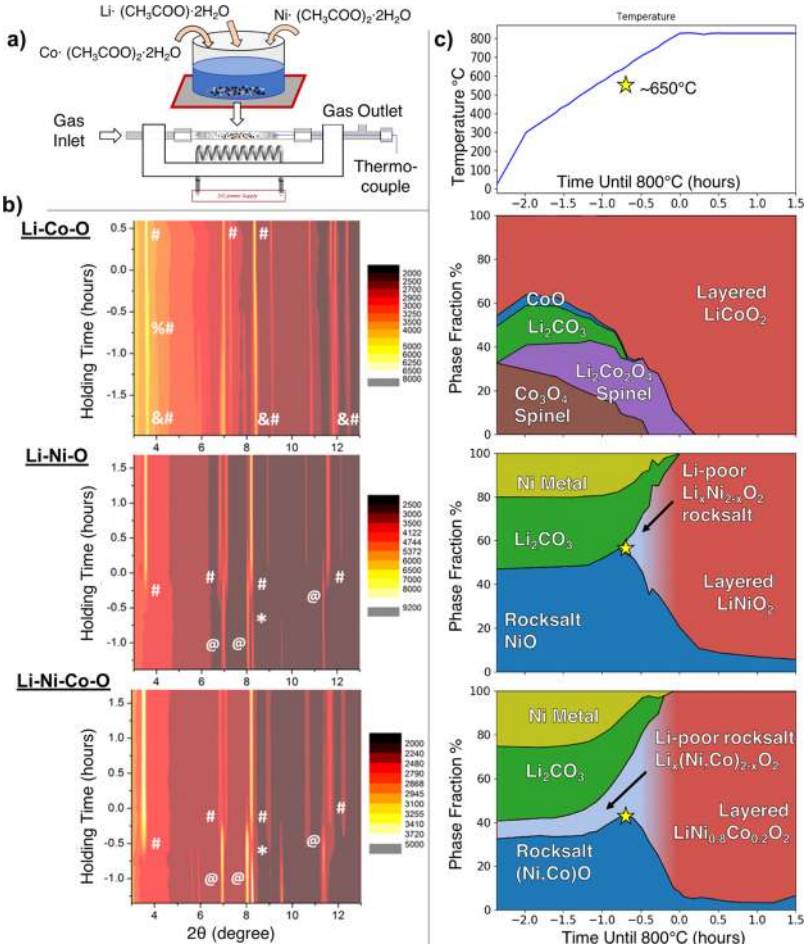

Figure 1. *In situ* tracking of intermediates during the solid-state synthesis of Co- and Ni-based layered oxides. (a) Schematic illustration of the two-step synthesis procedure, involving sol−gel processing of metal-acetate precursors (top) and then solid-state synthesis being characterized by *in situ* synchrotron XRD using a gas flow reactor (bottom). (b) Contour plots showing the evolution of XRD patterns during the synthesis of three different systems (Li−Co−O, Li−Ni−O, and Li−Ni−Co−O) as temperature ramps from room temperature to the holding temperatures of 775 °C for LNO and 825 °C for LCO and LNCO. Bragg peaks representing the major phases are marked with symbols: # layered oxides, & Co_3O_4, @ rocksalt (Ni/Co)O, and * Ni, % $Li_2Co_2O_4$-spinel. The full diffraction patterns in wide-angle ranges are provided in the Supporting Information (Figure S1). (c) Heating profile (top) and stack plots (bottom) for phase fractions of the detected crystalline phases, which are obtained from Rietveld refinements of *in situ* XRD data (see Figures S3 and S4 in the Supporting Information). In the heating profile, the heating time is set as 0 at the beginning of constant-temperature holding.

sensitive to synthetic conditions, such as heating temperature, time, and environment.[19,20]

The formation and persistence of these nonequilibrium phases are likely correlated with the structural defects associated with suboptimal battery performance. However, it is difficult to ascertain the origin of these nonequilibrium phases, as synthesis in the lab is typically operated in a sealed "black-box" reactor, where interpretation of cause-and-effect during synthesis optimization is informed by post-mortem analysis *via ex situ* characterization. High-energy synchrotron X-ray diffraction (XRD) is becoming a powerful tool to monitor the structural changes and phase evolution of battery materials during chemical and electrochemical reactions[14,21,22] and has also been recently applied to *in situ* studies of the synthesis of solid-state materials.[23−26] The high X-ray flux of the synchrotron light source allows high-quality full-range XRD patterns to be taken on a time scale of seconds, and therefore, the fast and subtle changes in the structure and composition can be followed. Herein, *in situ* synchrotron XRD is applied to study the solid-state synthesis of layered oxides, LCO and LNO, and the high-Ni solid-solution, $LiNi_{0.8}Co_{0.2}O_2$ (LNCO) being chosen because of its technological relevance to the battery application. We investigate a common solid-state synthesis route, whereby metal salt precursors are initially mixed into an aqueous slurry, which is then dried and calcined to high temperatures.

We find that the disordered and nonequilibrium phases that are observed in the early stages of high-temperature calcination are structurally related to stable binary oxides resulting from the decomposition of the metal-salt precursors. Structural evolution is thereby topotactically templated by LT intermediates which form during the early stages of crystallization. While this is of direct interest toward the synthetic control of structural ordering in battery materials, these insights also provide general principles toward understanding structure-selection mechanisms and controlling the formation of solid-state inorganic materials *via* precursor manipulation. For example, it is becoming increasingly possible to computationally predict which nonequilibrium intermediates form during aqueous precipitation.[27,28] Our work here provides a valuable conceptual framework to approach synthesis-by-design,[29] whereby manipulating precursors to produce initial phases

https://dx.doi.org/10.1021/acs.chemmater.0c02568
Chem. Mater. 2020, 32, 9906−9913

with desirable structural motifs, one can direct structural evolution down specific crystallization pathways toward the synthesis of target phases and structural properties.

2. EXPERIMENTS AND CALCULATIONS

2.1. *In Situ* Characterization of Solid-State Synthesis. *In situ* XRD measurements were conducted at beamline F2 at the Cornell High Energy Synchrotron Source (CHESS). The X-ray wavelength was 0.29526 Å. The XRD patterns were collected using a GE area detector (pixel size: 200 × 200 μm^2). For the *in situ* XRD measurements, the samples were prepared through a sol−gel like aqueous treatment by dissolving acetate-based precursors $Ni(CH_3COO)_2{\cdot}4H_2O$, $Co(CH_3COO)_2{\cdot}4H_2O$, and $CH_3COOLi{\cdot}2H_2O$ at a certain molar ratio into distilled water under magnetic stirring at 80 °C. An extra 3% of lithium source ($CH_3COOLi{\cdot}2H_2O$) was used in order to compensate for the volatility of lithium at high heating temperatures. The resulting solution was then continuously stirred to evaporate the solvent and subsequently dried in vacuum at 120 °C for 12 h. For the synthesis of LCO, LNO, and LNCO, the molar ratios between Ni and Co sources in the precursors were 0:1, 1:0, and 0.8:0.2, respectively. Prior to the *in situ* measurements, the precursors were preheated in a tube furnace with continuous oxygen flow for 10 h at 300 °C for the synthesis of LCO and 400 °C for the synthesis of LNO and LNCO. During the preheat treatment, the acetate precursors went through thermal decomposition, giving rise to mass loss as reported in previous studies *via* thermogravimetric analysis.[14] The compositions of the crystalline phases after the preheating were determined by XRD and quantitative phase analysis by Rietveld refinement (as given in Supporting Information; Table S1 and Note S1).

A gas flow reactor, as illustrated in Figure 1a, was used for the *in situ* XRD measurements. The powder samples (after preheat treatment) were loosely filled in a thin-walled sapphire tube attached to a stainless fixture with Swagelok fittings and graphite ferrules. Quartz wool was inserted in the tube from both ends to prevent the powders from moving under gas flow. A Kanthal (FeCrAl) alloy coil was mounted beneath the sapphire tube to heat the sample with electricity provided by a DC power supply. A k-type thermocouple was inserted from one end of the tube into the quartz wool to monitor the temperature and to feed back to the temperature controller. A temperature calibration curve was established by using ceria (CeO_2) powder as the thermal expansion standard. The temperature of the reactor was raised in a three-step ramping profile: first, quickly ramped up to about 300 °C, followed by a slow ramp to the desired reaction temperatures, and then maintained at the temperature for a period of time. The XRD patterns were taken at a time interval of about 4 min during the slow ramping and the constant temperature period, with 10 s counting time for each pattern. Industrial grade (99.5%) oxygen was continuously flowing through the reactor during the *in situ* XRD measurements.

Quantitative analysis with Rietveld refinement was conducted using TOPAS-5 (Bruker AXS). Details on the refinements are provided in the Supporting Information Note S1, Table S2, and Figure S5, with the examples for the preheated precursors. Same procedures were taken in refining the individual patterns from *in situ* XRD measurements.

2.2. *Ab Initio* Calculations. Crystal structures for intermediates $Li_{1-x}Ni_xO_2$ were obtained from cluster expansion calculations in the Li−Ni−Vac−O space, calculated previously in ref 37 using the methods described therein. Simulated XRD patterns for $Li_{1-x}Ni_xO_2$ were computed using the Pymatgen package.[30]

3. RESULTS

3.1. Kinetic Pathways toward Forming Layered Oxides. Precursors for synthesizing LCO, LNO, and LNCO were made by sol−gel processing of metal-acetate precursors (Figure 1a, top) followed by preheat treatment (as described in the Experiments and Calculations). Following previous studies on the early stage preheat process,[14] solid-state synthesis, starting with preheated powders, was conducted *in situ* under synchrotron XRD characterization using a flow cell (Figure 1a; bottom), following the heating profile given in Figure 1 (top). Figures S1 and 1b show the representative *in situ* XRD patterns taken during calcination in the wide-angle and selected ranges, respectively, allowing identification of all major phases (with corresponding Bragg peaks marked by symbols). Through quantitative Rietveld refinement, the phase evolution in the Li−Co−O, Li−Ni−O, and Li−Ni−Co−O systems as a function of time and temperature was extracted, as shown in Figure 1c. *In situ* XRD patterns taken at selected temperatures during the synthesis are presented in Figures S2−S4, showing the contributions of individual phases to the subtle XRD features, such as asymmetric shoulders.

3.1.1. Li−Co−O. As shown in Table S1, the phase fractions following the aqueous slurry and preheat treatment of Li-acetate and Co-acetate is 43.4% layered LCO, 34.9% spinel Co_3O_4, 17.1% Li_2CO_3, and 4.6% rocksalt CoO ($Fm\bar{3}m$). As shown in Figure 1c, immediately upon heating, a new phase is formed, which was resolved to correspond to spinel-type $Li_2Co_2O_4$—often referred to in the literature as LT-LCO.[31] The LT-LCO phase grows at the expense of CoO, Co_3O_4, and Li_2CO_3 and reaches a maximum phase fraction at 725 °C. At this point, CoO, Co_3O_4, and Li_2CO_3 are completely consumed. The LT-LCO phase fraction then declines with further temperature ramping, and concurrently, the layered LCO phase grows. The LT-LCO phase fully disappears after 36 min of isothermal sintering at 825 °C, after which no further structural changes were observed.

3.1.2. Li−Ni−O. The aqueous slurry and preheat treatment of Li-acetate and Ni-acetate resulted in 32.9% Li_2CO_3, 47.1% rocksalt NiO, and 19.9% Ni metal (Table S1). No layered ($R\bar{3}m$) LNO formed in the initial precursor treatment. During the *in situ* high-temperature calcining, the Li−Ni−O precursors were heated to 775 °C in 1.75 h and then held for approximately 2.5 h (Figure 1b). As shown in Figure 1c, the phase fraction of NiO initially grows, while the Ni metal fraction decreases, indicating oxidation of the Ni metal. The phase fraction NiO grows up to 56% until 565 °C, after which LNO appears at about 624 °C and grows at the expense of NiO and Li_2CO_3. At 750 °C, Li_2CO_3 is fully consumed, and the growth of LNO stops. A minority fraction of rocksalt NiO coexists with LNO even at the end of the sintering process.

3.1.3. Li−Ni−Co−O. In preparing for the synthesis of LNCO, Li-acetate, Co-acetate, and Ni-acetate precursors were mixed aqueously at a 1.0:0.8:0.2 ratio, resulting in a preheat treatment with 7.3 layered LNCO, 34.1% Li_2CO_3, 33.3% rocksalt (Ni,Co)O, and 25.3% Ni metal (Table S1). The composition of the rock salt NiO−CoO solid solution was determined from its lattice parameter *a*, which was refined to be 4.1876(1) Å, corresponding to a $Ni_xCo_{1-x}O$ solid-solution with x = 0.85.[32] As shown in Figure 1c, there is about 8%

https://dx.doi.org/10.1021/acs.chemmater.0c02568
Chem. Mater. 2020, 32, 9906−9913

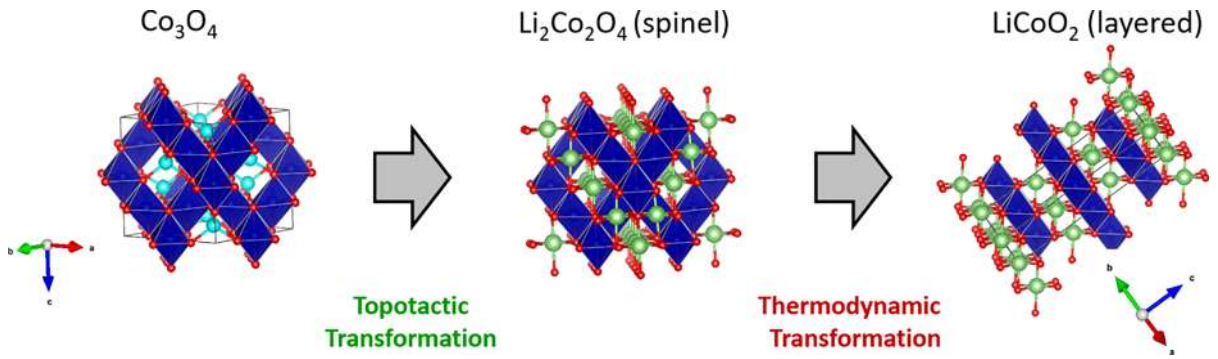

Figure 2. Transformation pathways during the synthesis of layered $LiCoO_2$. Formation of metastable spinel $Li_2Co_2O_4$ proceeds *via* topotactic transformation from spinel Co_3O_4, driven by a kinetically facile Li^+/Co^{2+} exchange reaction. The transformation from the spinel $Li_2Co_2O_4$ to layered $LiCoO_2$ is thermodynamically driven, involving local Co^{3+} ion-migration (as illustrated).

layered $Li(Co,Ni)O_2$ present in the sample following the preheat treatment. The rock salt (Ni,Co)O component grows to a maximum phase fraction of 43% at 650 °C, before transformation into the layered $LiNi_{0.8}Co_{0.2}O_2$. Below 700 °C, the LNCO layered phase has a lower c/a ratio than is expected for an $R\bar{3}m$ layered structure. We will show that this corresponds to a disordered Li-deficient nonstoichiometric phase $Li_{1-x}(Ni,Co)_xO_2$ with interlayer Li/Ni mixing, which eventually transforms to near-stoichiometric layered $LiNi_{0.8}Co_{0.2}O_2$ at temperatures above 700 °C.

3.2. Formation of Metastable Spinel $Li_2Co_2O_4$ Prior to Layered LCO. Spinel $Li_2Co_2O_4$ is usually obtained when LCO is synthesized under 400 °C,[8,10,11] resulting in its description as the "LT" polymorph of LCO in contrast to the "high-temperature" layered LCO phase. From thermodynamics, an LT phase has lower enthalpy and lower entropy than the higher-temperature (HT) polymorph. From the LT/HT-LCO nomenclature, one could reasonably assume that there is a first-order thermodynamic phase transition between spinel $Li_2Co_2O_4$ and layered LCO with a transition temperature around 400 °C.

Our *in situ* experiments appear to contradict this nomenclature for two reasons. First, spinel $Li_2Co_2O_4$ is not present at the beginning of the *in situ* synthesis experiment, even though all samples were prepared at temperatures below 400 °C. Second, during high-temperature calcination, the phase fraction of $Li_2Co_2O_4$ continues to grow up until 725 °C, which is much higher than the anticipated crossover temperature (400 °C, as reported in literature).[9] These results suggest that the nomenclature implied by "high-temperature" and "LT" LCO may be misleading. This conclusion is supported by previous first-principles density functional theory (DFT) calculations of relative LCO polymorph phase stability, which show that the layered LCO phase has a lower enthalpy than the spinel $Li_2Co_2O_4$ phase,[12] and additional phonon calculations revealing that layered LCO also has higher entropy than spinel $Li_2Co_2O_4$.[13] These free-energy calculations indicate that spinel $Li_2Co_2O_4$ is metastable with respect to layered LCO at all temperatures, although it is only metastable by 8 to 20 meV/formula, which is small compared to other metastable inorganic compounds.[33]

Our *in situ* synchrotron study reveals that the growth of spinel $Li_2Co_2O_4$ occurs primarily at the expense of Co_3O_4. This implies that the formation of the metastable $Li_2Co_2O_4$ is kinetically driven by topotactic conversion from spinel Co_3O_4 in the presence of the lithium source.[34] Both $Li_2Co_2O_4$ and Co_3O_4 form in a spinel structure with space group $Fd\bar{3}m$ and possess frameworks of Co^{3+} octahedra compatible with each other. At 616 °C, the lattice parameters a of $Li_2Co_2O_4$ and Co_3O_4 are 8.0561 and 8.1104 Å, respectively, indicating that the unit cells can be coherent between these two phases. As illustrated in Figure 2, one-third of Co ions in Co_3O_4 are Co^{2+}, occupying a tetrahedral site in between the Co^{3+} layers. Octahedral Co^{3+} is immobile because of its high ligand field stabilization, but transformation of Co_3O_4 spinel to $Li_2Co_2O_4$ spinel can occur by out-diffusion of Co^{2+} and in-diffusion of Li^+.

These observations highlight the subtle competing effects between thermodynamics and kinetics in solid-state synthesis. Co_3O_4 is the equilibrium reaction product at LTs and templates the kinetically facile topotactic ion-exchange to metastable $Li_2Co_2O_4$. On the other hand, the high-temperature calcination provides the transformation kinetics required to drive the irreversible transformation of metastable spinel $Li_2Co_2O_4$ to the equilibrium layered LCO phase. As both polymorphs have the same composition, this transformation can proceed either by nucleation and growth or potentially by a cross-layer intermigration of Co and Li ions without any need for long-range diffusion.[35]

3.3. Formation of Nonstoichiometric, Disordered Rocksalts Prior to LNO/LNCO. In the synthesis of LNO and LNCO, the initial products from the decomposition of acetates consist of Li_2CO_3, Ni metal, and rocksalts NiO/(Ni,Co)O solid-solution. However, at temperatures below 700 °C, the lattice parameters of the layered $R\bar{3}m$ phase (being resolved from refinement) exhibit a surprisingly low c/a ratio < 4.899, as shown in Figure 3a. Only when temperatures are higher than 700 °C, does the c/a ratio increase to 4.899 and above.

The c/a ratio provides important clues about the structural ordering of the phases. In a perfect cubic rocksalt, such as NiO, the cubic lattice can be expressed in a hexagonal lattice such that $a_H = a_C/\sqrt{2}$ and $c_H = 2\sqrt{3}a_C$ with a c/a ratio of $2\sqrt{6} = 4.899$. In $R\bar{3}m$ layered transition-metal oxides, the c/a ratio is >4.899 because of the weak interlayer force, which results in a slight separation of the transition-metal layers along the c-axis. Therefore, the resolved lattice parameters of c/a ratio < 4.899 suggest a nontraditional layered or rocksalt intermediate compound, which was also observed in the synthesis of $LiNiO_2$ from NiO.[36] Through a combined Rietveld refinement and DFT investigation, we found that this resolved c/a ratio < 4.899 best corresponds to a disordered

https://dx.doi.org/10.1021/acs.chemmater.0c02568
Chem. Mater. 2020, 32, 9906−9913

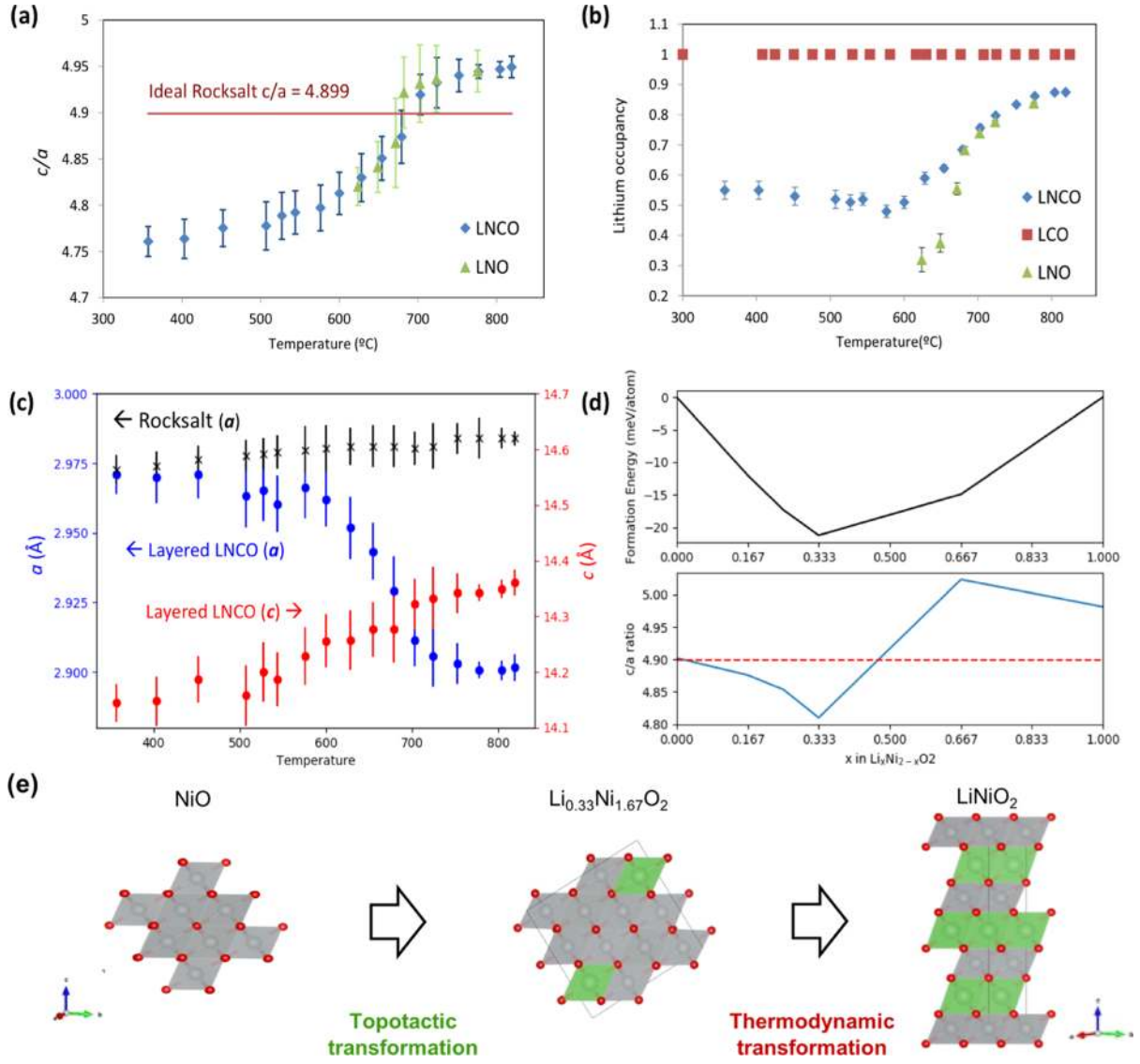

Figure 3. Transformation pathways during the synthesis of Ni-based layered oxides. (a) Deviation of the aspect ratio c/a to 4.899 (or $2\sqrt{6}$) in the intermediate structures of $Li_x(Co_{0.2}Ni_{0.8})_{1-x}O_2$ (LNCO) and $Li_xNi_{2-x}O_2$ (LNO). (b) Lithium occupancies at 3b sites in the layered structures as a function of temperature. (c) Comparisons of the lattice parameters a and c between the LNCO layered and rocksalt (Ni,Co)O. Error bars come from the microstrains estimated from the Bragg peak profiles of the LNCO and (Ni,Co)O phases. (d) DFT-calculated formation energies and c/a ratio in Li-deficient $Li_xNi_{2-x}O_2$ in the rocksalt structure (See also Figure S6 for the calculated XRD patterns). The minimum lattice parameter is found for $Li_{0.33}Ni_{1.67}O_2$. (e) Transformation pathways during the synthesis of $LiNiO_2$: formation of metastable $Li_{0.33}Ni_{1.67}O_2$ *via* topotactic transformation followed by thermodynamic transformation to the layered $LiNiO_2$ (as illustrated). (See also Figure S7 for the crystal structures of DFT-computed Li-deficient $Li_xNi_{2-x}O_2$ as prepared from ref 37).

$Li_x(Ni,Co)_{2-x}O_2$ rocksalt, where $x \sim 0.33$ for $LiNiO_2$ (Supporting Information, Note S2 and Figure S6). This Li-poor stoichiometry is supported by refinement of the Li-to-Ni occupancy ratio in the Li layer, as shown in Figure 3b. In contrast to the high stoichiometry (with 100% Li occupancy) in $LiCoO_2$ throughout the whole process, the Li occupancy in $Li_x(Ni,Co)_{2-x}O_2$ is low, only 0.3−0.5 below 650 °C and then increases gradually to ∼0.9 by 800 °C. The structure of the intermediate $Li_x(Ni,Co)_{2-x}O_2$ can be qualitatively viewed as a layered $R\bar{3}m$ structure with Ni substituted into the Li layer, or equivalently, as a rocksalt structure with Li substitutions on the Ni(Co) sites. The insertion of Li^+ into rocksalt is accompanied by $Ni^{2+}(Co^{2+})$ oxidation to $Ni^{3+}(Co^{3+})$. Subsequently, the smaller ion radius of 3+ cations shrinks the overall volume of this partially lithiated rocksalt phase, resulting in low c and high a lattice parameters and hence the small c/a ratio (<4.899), as shown in Figure 3c.

From Figure 1c, we see that the Li-poor disordered intermediate $Li_{0.33}Ni_{1.67}O_2$ forms at the expense of the NiO rocksalt precursor and transforms to the ordered $R\bar{3}m$ layered structure above 700 °C. In principle, the reaction of NiO with lithium could proceed through any intermediate composition in the Li−Ni−vacancy−O space.[37] Why specifically does this Li-deficient $Li_{0.33}Ni_{1.67}O_2$ compound form, which is clearly a nonequilibrium intermediate in a reaction vessel when the precursor stoichiometry totals to $LiNiO_2$? One notable aspect of $Li_{0.33}Ni_{1.67}O_2$ is that it is actually the deepest part of the binary convex hull in the isopleth among Li-deficient $Li_xNi_{2-x}O_2$, as shown in Figure 3d,e,or to put it another way, this $Li_{0.33}Ni_{1.67}O_2$ composition is the most exothermically

https://dx.doi.org/10.1021/acs.chemmater.0c02568
Chem. Mater. 2020, 32, 9906−9913

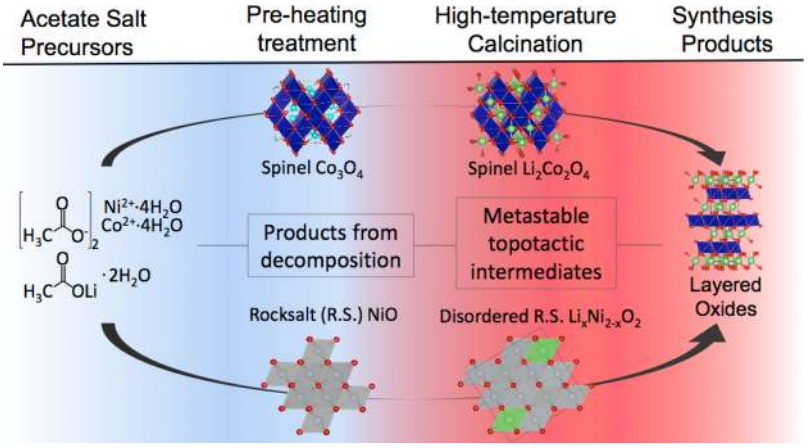

Figure 4. Schematic illustration of the *nonequilibrium* formation pathways of Co- and Ni-based layered oxides, templated by the LT intermediates. Structurally different metal oxides are formed from the decomposition of the Co-based (top) and Ni-based (bottom) acetate salt precursors (as highlighted in blue) and subsequently template the structural-evolution of *nonequilibrium* intermediates (in red). In the high-temperature calcination process, they all go through a topotactic process before turning into the thermodynamically stable layered phase ($R\bar{3}m$).

forming compound when rocksalt NiO reacts with the lithium source, which is consistent with the earlier observations on the presence of Ni vacancies in Ni slabs that may create space for cation migration and layering.[36]

The formation of $Li_{0.33}Ni_{1.67}O_2$ as an intermediate may be understood by considering the local boundary conditions of solid-state reaction. A chemical reaction between two precursor powders occurs at their shared interface.[38] Locally, the powders have no knowledge of the total stoichiometric composition of the system. Therefore, the composition that forms in this interfacial reaction does not necessarily need to be the compound corresponding to the ratios of the prepared precursors. Rather, the first compound to form at the interface should be the one whose reaction free-energy is the most exothermic.[39] We note that while this "maximum reaction-energy" compound would be a nonequilibrium intermediate from the perspective of the total stoichiometry of the precursors, it is a *stable* intermediate in the interfacial reaction between powder precursors. This nonequilibrium compound would then react with excess precursors to eventually evolve to the equilibrium target composition. Such a phenomenon is not exclusive to the lithium compounds but has already been observed in the sodium ones (Na_xCoO_2 and Na_xMnO_2).[38] We propose that this 'maximum pairwise reaction-energy' concept, originally proposed to explain reaction products in solid-state formation of sodium compounds and solid electrolyte/electrode interfaces,[40] may be a general principle behind the formation of nonequilibrium intermediates during solid-state reactions.

When heated to temperatures above 700 °C, the ordered layered $Li(Ni,Co)O_2$ phase appears prominently as Li ions are found to occupy >80% of 3b sites, and the c/a ratio increases from the cubic limit of 4.899. This process is synchronized with the depletion of Ni(Co)O and Li_2CO_3, as shown in Figure 1, suggesting the formation of layered phase. Our lattice parameter investigation suggests that LNO and LNCO both form *via* phase transition from a Li-poor, Ni-rich disordered rocksalt phase to a near-stoichiometric layered phase at temperatures above 700 °C. It is notable that the non-equilibrium intermediate is observable only in *in situ* measurements as *ex situ* data taken from samples heated at 500 °C for 10 h show a c/a ratio well above $2\sqrt{6}$ (Figure 3a), demonstrating that $Li_x(Ni,Co)_{2-x}O_2$ is truly a transient intermediate.

The measured c/a ratios of LNO and LNCO in Figure 3a match up closely. So, even though we have not resolved the phase diagram of the quinary Li−Ni−Co−vacancy−O space, it is reasonable to assume that the Li-poor intermediate in the LNCO system is similar to the one in the LNO system. One notable difference is that the Li-deficient intermediate appears in the LNO system only at temperatures above ∼650 °C, but it appears in the LNCO system immediately after preheat treatment of acetates. As measured by calorimetry, LCO has a more exothermic formation enthalpy than LNO, while their mixing enthalpies are nearly ideal;[7] this suggests that Co incorporation into LNO could play a stabilizing effect to the lower formation temperature of the disordered rocksalt, $Li_x(Ni,Co)_{2-x}O_2$, with plausibly a higher Li concentration ($x \sim 0.5$) as suggested by the refinement results (Figure 3b).

In summary, based on quantitative *in situ* characterization supported by DFT structure analysis, we propose a two-step reaction mechanism where layered LNO and LNCO are formed *via* a nonstoichiometric (Li-deficient nickel-rich) rocksalt $Li_x(Ni,Co)_{2-x}O_2$ below 700 °C, which then transforms into an idealized layered phase above 700 °C. The lithium-deficient compound is the most exothermically forming compound in the interfacial reaction between Li_2CO_3 and NiO; this principle governs the structure selection of the nonequilibrium intermediate which forms in this reaction. At high temperatures, this phase reacts with the remaining lithium to evolve to the equilibrium LNO and LNCO composition over time.

4. DISCUSSION AND OUTLOOK

From this study we demonstrated that a combination of *in situ* quantitative analysis and *ab initio* calculations provides access to the kinetic pathways during solid-state synthesis, involving metastable intermediates prior to forming the final equilibrium phases. For the specific case in the synthesis of layered oxides, the kinetic pathways are summarized in Figure 4. Although both Ni- and Co-based layered oxides ultimately crystallize into the same thermodynamically stable $R\bar{3}m$ layered structure, they evolve through different metastable intermediates on the way to the final equilibrium products. LCO intermediate

https://dx.doi.org/10.1021/acs.chemmater.0c02568
Chem. Mater. 2020, 32, 9906−9913

phases are primarily dominated by a metastable spinel structural motif with the same stoichiometry, whereas the LNO and LNCO intermediates proceed through a disordered rocksalt structural motif, or to put it another way, the structural evolution during high-temperature solid-state synthesis is not necessarily governed by a slow formation and further structural transformation to the reaction end-product, as is commonly assumed. Rather, material formation proceeds through a series of well-defined phases, including phases that are thermodynamically stable in other parts of the composition space (e.g., Co_3O_4), combined with kinetically facile topotactic transformations, if such pathways are available. Because the metastable spinel $Li_2Co_2O_4$ polymorph and disordered non-stoichiometric $Li_{1-x}(Ni,Co)_xO_2$ phases are kinetic lithiation byproducts from these initial binary oxides, the formation and persistence of these intermediates to high temperatures may be the origin of the well-known structural defects that plague the electrochemical performance of layered oxide cathode materials. Therefore, the observations may explain the common observations of the preferential off-stoichiometry and high Li/Ni mixing in $LiNiO_2$ and high-Ni layered oxides but not in Co-based ones.[17,41]

By rationalizing the mechanisms driving the formation of nonequilibrium intermediates during solid-state synthesis, we can more rationally design the early-stage processing or manipulation of precursors toward targeted structural motifs. For example, in Co-based systems, synthesis of LCO *via* $Co(OH)_2$, a layered cobalt hydroxide phase, can provide a lithiation structural template for LCO at much lower temperatures and shortened synthesis time than synthesis from binary oxide precursors.[42] Likewise, coprecipitation through layered double hydroxides is now the industrially adopted route toward the synthesis of advanced $Li(Ni_xMn_yCo_z)O_2$ battery cathode materials as these are isostructural to the target compound.[43]

These general principles involving the structure selection and phase evolution through nonequilibrium intermediates apply beyond layered oxides, as was previously demonstrated in the synthesis of $Li_3V_2(PO_4)_3$ (LVP) through a hydrothermal-assisted approach. In that case, a hydrothermal processing step was added prior to solid-state synthesis to form an amorphous intermediate with local structural resembling to that of the final product. The pathway through this intermediate was found to be crucial to form nanocrystalline LVP with excellent cycling stability and rate capability.[44] By controlling the synthesis conditions to precipitate precursor phases with desired structural motifs, we can bias kinetically facile topotactic transformations from these initial intermediates. Being able to rationally navigate these nonequilibrium crystallization pathways will provide new opportunities to design predictive strategies for synthesizing advanced functional materials.

■ ASSOCIATED CONTENT

Supporting Information

The Supporting Information is available free of charge at https://pubs.acs.org/doi/10.1021/acs.chemmater.0c02568.

Composition of crystalline phase in the precursors for in situ XRD measurement, phase identification of the intermediates during synthesis of LCO, LNCO, structure of the LCO and LNCO disordered compound, and simulated XRD patterns of the DFT-computed $Li_xNi_{2-x}O_2$ isopleth (PDF)

■ AUTHOR INFORMATION

Corresponding Authors

Gerbrand Ceder − *Materials Sciences Division, Lawrence Berkeley National Laboratory, Berkeley, California 94704, United States; Department of Materials Science and Engineering, UC Berkeley, Berkeley, California 94720, United States;* orcid.org/0000-0001-9275-3605; Email: gceder@berkeley.edu

Feng Wang − *Sustainable Energy Technologies Department, Brookhaven National Laboratory, Upton, New York 11973, United States;* orcid.org/0000-0003-4068-9212; Email: fwang@bnl.gov

Authors

Jianming Bai − *National Synchrotron Light Source II, Brookhaven National Laboratory, Upton, New York 11973, United States;* orcid.org/0000-0002-0575-2987

Wenhao Sun − *Materials Sciences Division, Lawrence Berkeley National Laboratory, Berkeley, California 94704, United States;* orcid.org/0000-0002-8416-455X

Jianqing Zhao − *Sustainable Energy Technologies Department, Brookhaven National Laboratory, Upton, New York 11973, United States*

Dawei Wang − *Sustainable Energy Technologies Department, Brookhaven National Laboratory, Upton, New York 11973, United States*

Penghao Xiao − *Materials Sciences Division, Lawrence Berkeley National Laboratory, Berkeley, California 94704, United States*

Jun Young Peter Ko − *The Cornell High Energy Synchrotron Source, Cornell University, Ithaca, New York 14853, United States*

Ashfia Huq − *Neutron Sciences Division, Oak Ridge National Laboratory, Oak Ridge, Tennessee 37831, United States*

Complete contact information is available at: https://pubs.acs.org/10.1021/acs.chemmater.0c02568

Author Contributions

J.B. and W.S. contributed equally. The manuscript was written through contributions of all authors. All authors have given approval to the final version of the manuscript.

Notes

The authors declare no competing financial interest.

■ ACKNOWLEDGMENTS

This work was funded by the US Department of Energy, Office of Science, Basic Energy Sciences, under contract no. UGA-0-41029-16/ER392000 as a part of the DOE Energy Frontier Research Center "Center for Next Generation of Materials Design: Incorporating Metastability." Experimental work is partially supported by the U.S. Department of Energy (DOE) Office of Energy Efficiency and Renewable Energy, Vehicle Technologies Office, contract no. DE-SC0012704. Synchrotron X-ray measurements carried out at the National Synchrotron Light Source II of Brookhaven National Laboratory were supported by the U.S. Department of Energy, Office of Basic Energy Sciences under contract no. DE-SC0012704. The *in situ* synchrotron XRD work was conducted at the Cornell High Energy Synchrotron Source (CHESS), which is supported by the National Science Foundation and

the National Institutes of Health/National Institute of General Medical Sciences under NSF award DMR-1332208.

REFERENCES

(1) Goodenough, J. B.; Park, K.-S. The Li-ion rechargeable battery: a perspective. *J. Am. Chem. Soc.* **2013**, *135*, 1167.
(2) Whittingham, M. S. Ultimate limits to intercalation reactions for lithium batteries. *Chem. Rev.* **2014**, *114*, 11414.
(3) Ceder, G.; et al. Identification of cathode materials for lithium batteries guided by first-principles calculations. *Nature* **1998**, *392*, 694.
(4) Yabuuchi, N.; Ohzuku, T. Novel lithium insertion material of $LiCo_{1/3}Ni_{1/3}Mn_{1/3}O_2$ for advanced lithium-ion batteries. *J. Power Sources* **2003**, *119-121*, 171.
(5) Liu, W.; et al. Nickel-rich layered lithium transition-metal oxide for high-energy lithium-ion batteries. *Angew. Chem., Int. Ed.* **2015**, *54*, 4440.
(6) Radin, M. D.; et al. Narrowing the gap between theoretical and practical capacities in Li-Ion layered oxide cathode materials. *Adv. Energy Mater.* **2017**, *7*, 1602888.
(7) Wang, M.; Navrotsky, A. Enthalpy of formation of LiNiO2, LiCoO2 and their solid solution, LiNi1− xCoxO2. *Solid State Ionics* **2004**, *166*, 167.
(8) Gummow, R.; et al. Structure and electrochemistry of lithium cobalt oxide synthesized at 400 °C. *Mater. Res. Bull.* **1992**, *27*, 327.
(9) Gummow, R.; Thackeray, M. M. Lithium cobalt nickel-oxide cathode materials prepared at 400°C for rechargeable lithium batteries. *Solid State Ionics* **1992**, *53-56*, 681.
(10) Rossen, E.; Reimers, J.; Dahn, J. Synthesis and electrochemistry of spinel LT- $LiCoO_2$. *Solid State Ionics* **1993**, *62*, 53.
(11) Garcia, B.; et al. Electrochemical properties of low temperature crystallized $LiCoO_2$. *J. Electrochem. Soc.* **1997**, *144*, 1179.
(12) Wolverton, C.; Zunger, A. Prediction of Li intercalation and battery voltages in layered vs. cubic Li_xCoO_2. *J. Electrochem. Soc.* **1998**, *145*, 2424.
(13) Kim, S.; et al. First-principles study of lithium cobalt spinel oxides: correlating structure and electrochemistry. *ACS Appl. Mater. Interfaces* **2018**, *10*, 1347.
(14) Zhao, J.; et al. *In Situ* probing and synthetic control of cationic ordering in Ni-rich layered oxide cathodes. *Adv. Energy Mater.* **2017**, *7*, 1601266.
(15) Kang, K.; Ceder, G. Factors that affect Li mobility in layered lithium transition metal oxides. *Phys. Rev. B: Condens. Matter Mater. Phys.* **2006**, *74*, 094105.
(16) Kalyani, P.; Kalaiselvi, N. Various aspects of $LiNiO_2$ chemistry: a review. *Sci. Technol. Adv. Mater.* **2005**, *6*, 689.
(17) Zhang, M.-J.; et al. Cationic ordering coupled to reconstruction of basic building units during synthesis of high-Ni layered oxides. *J. Am. Chem. Soc.* **2018**, *140*, 12484.
(18) Wang, D.; et al. Intrinsic role of cationic substitution in tuning Li/Ni mixing in high-Ni layered oxides. *Chem. Mater.* **2019**, *31*, 2731.
(19) Gover, R. K. B.; et al. Effects of sintering temperature on the structure of the layered phase $Li_x(Ni_{0.8}Co_{0.2})O_2$. *J. Electrochem. Soc.* **2000**, *147*, 4045.
(20) Jouybari, Y. H.; Asgari, S. Synthesis and electrochemical properties of $LiNi_{0.8}Co_{0.2}O_2$. nanopowders for lithium ion battery applications. *J. Power Sources* **2011**, *196*, 337.
(21) Wang, D.; et al. Synthetic control of kinetic reaction pathway and cationic ordering in high-Ni layered oxide cathodes. *Adv. Mater.* **2017**, *29*, 1606715.
(22) Glazer, M. P. B.; et al. High-energy x-ray scattering studies of battery materials. *MRS Bull.* **2016**, *41*, 460.
(23) Bai, J.; et al. Solvothermal synthesis of $_{LiMn1-x}Fe_xPO_4$ cathode materials: a study of reaction mechanisms by time-resolved in situ synchrotron X-ray diffraction. *J. Phys. Chem. C* **2015**, *119*, 2266.
(24) Shoemaker, D. P.; et al. In situ studies of a platform for metastable inorganic crystal growth and materials discovery. *Proc. Natl. Acad. Sci. U.S.A.* **2014**, *111*, 10922.
(25) Martinolich, A. J.; Neilson, J. R. Toward reaction-by-design: achieving kinetic control of solid state chemistry with metathesis. *Chem. Mater.* **2017**, *29*, 479.
(26) Chen, B.-R.; et al. Understanding crystallization pathways leading to manganese oxide polymorph formation. *Nat. Commun.* **2018**, *9*, 2553.
(27) Sun, W.; et al. Nucleation of metastable aragonite CaCO3 in seawater. *Proc. Natl. Acad. Sci. U.S.A.* **2015**, *112*, 3199.
(28) Sun, W.; et al. Non-equilibrium crystallization pathways of manganese oxides in aqueous solution. *Nat. Commun.* **2019**, *10*, 573.
(29) Stein, A.; Keller, S. W.; Mallouk, T. E. Turning down the heat: Design and mechanism in solid-state synthesis. *Science* **1993**, *259*, 1558.
(30) Ong, S. P.; et al. Python Materials Genomics (pymatgen): a robust, open-source python library for materials analysis. *Comput. Mater. Sci.* **2013**, *68*, 314.
(31) Rossen, E.; Reimers, J.; Dahn, J. Synthesis and electrochemistry of spinel LT- $LiCoO_2$. *Solid State Ionics* **1993**, *62*, 53.
(32) Kuboon, S.; Hu, Y. H. Study of NiO−CoO and Co_3O_4− Ni_3O_4 solid solutions in multiphase Ni−Co−O systems. *Ind. Eng. Chem. Res.* **2011**, *50*, 2015.
(33) Sun, W.; et al. The thermodynamic scale of inorganic crystalline metastability. *Sci. Adv.* **2016**, *2*, No. e1600225.
(34) Wicker, S. A.; Walker, E. H. Revisited: decomposition or melting? formation mechanism investigation of LiCoO2 via in situ time-resolved X-ray diffraction. *Inorg. Chem.* **2013**, *52*, 1772.
(35) Kan, Y.; et al. Differentiating allotropic LiCoO2/Li2Co2O4: A structural and electrochemical study. *J. Power Sources* **2014**, *271*, 97.
(36) Bianchini, M.; Fauth, F.; Hartmann, P.; Brezesinski, T.; Janek, J. An in situ structural study on the synthesis and decomposition of $LiNiO_2$. *J. Mater. Chem. A* **2020**, *8*, 1808.
(37) Das, H.; et al. First-Principles simulation of the (Li−Ni−vacancy)O phase diagram and its relevance for the surface phases in Ni-rich Li-ion cathode materials. *Chem. Mater.* **2017**, *29*, 7840.
(38) Bianchini, M.; et al. The interplay between thermodynamics and kinetics in the solid-state synthesis of P2 layered oxides. *Nat. Mater.* **2020**, *19*, 1088.
(39) Walser, R. M.; Bené, R. W. First phase nucleation in silicon-transition-metal planar interfaces. *Appl. Phys. Lett.* **1976**, *28*, 624.
(40) Richards, W. D.; et al. Interface stability in solid-state batteries. *Chem. Mater.* **2015**, *28*, 266.
(41) Zheng, J.; et al. Ni/Li disordering in layered transition metal oxide: electrochemical impact, origin, and control. *Acc. Chem. Res.* **2019**, *52*, 2201.
(42) Huang, B.; et al. Electrochemical evaluation of $LiCoO_2$ synthesized by decomposition and intercalation of hydroxides for lithium-ion battery applications. *J. Appl. Electrochem.* **1998**, *28*, 1365.
(43) Shin, Y.; et al. Investigation on the microscopic features of layered oxide $Li[Ni_{1/3}Co_{1/3}Mn_{1/3}]O_2$ and their influences on the cathode properties. *Solid State Ionics* **2006**, *177*, 515.
(44) Wang, L.; et al. Structure tracking aided design and synthesis of $Li_3V_2(PO_4)_3$ nanocrystals as high-power cathodes for lithium ion batteries. *Chem. Mater.* **2015**, *27*, 5712.

https://dx.doi.org/10.1021/acs.chemmater.0c02568
Chem. Mater. 2020, 32, 9906−9913